



ELSEVIER

Isopycnal displacements within the Cape Basin thermocline as revealed by the Hydrographic Data Archive

Claudia F. Giulivi*, Arnold L. Gordon

Lamont-Doherty Earth Observatory of Columbia University, Division of Ocean and Climate Physics, 61 Route 9W, Palisades, NY 10964, USA

Received 20 April 2005; received in revised form 12 May 2006; accepted 20 May 2006

Abstract

The transfer of upper kilometer water from the Indian Ocean into the South Atlantic, the Agulhas leakage, is believed to be accomplished primarily through meso-scale eddy processes. There have been various studies investigating eddies of the “Cape Basin Cauldron” from specific data sets. The hydrographic data archive acquired during the last century within the Cape Basin region of the South Atlantic provides additional insight into the distribution and water mass properties of the Cape Basin eddies. Eddies are identified by mid-thermocline isopycnal depth anomalies relative to the long-term mean. Positive depth anomalies (the reference isopycnal is deeper than the long-term mean isopycnal depth) mark the presence of anticyclonic eddies; negative anomalies mark cyclonic eddies. Numerous eddies are identified in the whole region; the larger isopycnal displacements are attributed to the energetic eddies characteristic of the Cape Basin and indicate that there is a 2:1 anticyclone/cyclone ratio. Smaller displacements of the less energetic features are almost equally split between anticyclones and cyclones (1.4:1 ratio). Potential temperature, salinity and oxygen relationships at thermocline and intermediate levels within each eddy reveal their likely origin. The eddy core water is not solely drawn from Indian Ocean: tropical and subtropical South Atlantic water are also present. Anticyclones and cyclones carrying Agulhas Water properties are identified throughout the Cape Basin. Anticyclones with Agulhas Water characteristics show a predominant northwest dispersal, whereas the cyclones are identified mainly along the western margin of the African continent, possibly related to their origin as shear eddies at the boundary between the Agulhas axis and Africa. Cyclones and anticyclones carrying pure South Atlantic origin water are identified south of 30°S and west of the Walvis Ridge. Tropical Atlantic water at depth is found for cyclones north of the Walvis Ridge, west of 10°E and for stations deeper than 4000 m, and a few anticyclones with the same characteristics are found south of the ridge.

© 2006 Elsevier Ltd. All rights reserved.

Keywords: Agulhas Current system; Water masses; Hydrography; Thermocline water; Intermediate water; Oceanic eddies; Retroflexion; The Southeast Atlantic Ocean (10°W–21°E; 20°–41°S)

1. Introduction

The transfer of Indian Ocean water into the upper kilometer of the South Atlantic at the Agulhas Retroflexion, or what is commonly referred to as the Agulhas leakage, has attracted considerable

*Corresponding author. Tel.: +1 845 365 8576;
fax: +1 845 365 8157.

E-mail address: claudiag@ldeo.columbia.edu (C.F. Giulivi).

interest, particularly in the last two decades (Lutjeharms, 1996; Gordon et al., 1999). One of the reasons for this extensive research is the significance of the Agulhas leakage in maintaining the global thermohaline overturning circulation associated with the export of North Atlantic Deep Water (NADW), through the so-called warm-route (Gordon, 1986, 1996, 2003; Gordon et al., 1992; de Ruijter et al., 1999). Mesoscale eddies or rings formed from western boundary currents can be found all over the world. Large, energetic mesoscale eddies (>100 km) spun-off western boundary currents are often called rings (e.g. Gulf Stream, Kuroshio and Brazil Current Rings). Agulhas rings shed into the Cape Basin have a diameter of about 200 km, anticyclonic rotation and a distinct core (Van Veldhoven, 2005). Cold-core (cyclonic) eddies have also been observed in the area of the Agulhas Retroflection and Cape Peninsula. These coexist with the anticyclones but have smaller diameter (~120 km) and drift across the northwestward migration path of the anticyclones (Hardman-Mountford et al., 2003). Agulhas eddies or rings shed from the Agulhas Retroflection, which may be the primary means of the transfer of the Atlantic–Indian Ocean thermocline water, drift into the Cape Basin inducing a vigorous field of meso-scale fluctuations (Duncombe Rae, 1991; Byrne et al., 1995; Lutjeharms, 1996; de Ruijter et al., 1999). To this transfer of water we have to add the contributions from the direct leakage of Agulhas Water into the South Atlantic (Gordon, 1985; Gordon et al., 1987) and from current filaments (Lutjeharms and Cooper, 1996). These various inputs of water make the Retroflection act as a “valve” regulating the buoyancy of water in the upper kilometer of the South Atlantic Ocean and may in turn regulate NADW overturning (Gordon, 2003).

The Agulhas leakage history during the past 550,000 years was investigated from a sediment record in the Cape Basin (Peeters et al., 2004). The results show that the Indian–Atlantic Ocean water exchange was highly variable, enhanced during present and past interglacials and reduced during glacial intervals. The onset of increased Agulhas leakage during late glacial conditions suggests a crucial role for Agulhas leakage in glacial terminations, the timing of interhemispheric climate change and the resumption of the Atlantic thermohaline circulation and NADW formation.

Hydrographic and tracer data show that the westward transfer of Indian Ocean water into the

southeast Atlantic is limited to water with potential densities with respect to the sea surface, lower than 27.5 and shallower than 1500–2000 m (Gordon et al., 1992). At greater depths, the water flowing within the Retroflection pattern consists primarily of Atlantic and Circumpolar Deep Water (Gordon et al., 1987). Agulhas eddies display hydrographic contrasts with the ambient waters of the southeast Atlantic Ocean, being generally warmer and saltier as measured along isopycnals. Fluid particles may be trapped in, and thus advect with, a flow disturbance such as an eddy, or oscillate in position as an eddy passes; the trapping depth will depend on the relationship between the translation and swirl speeds of the eddy (Flierl, 1981). Duncombe Rae (1991) demonstrated that for the observed Agulhas rings the deepest presence of trapped Indian Ocean water lies between 1100 and 670 m, encompassing the surface, thermocline and intermediate water masses. Results from a numerical, isopycnal ocean model (de Steur et al., 2004) show that heat and salt anomalies associated with Agulhas rings are entrained within the upper branch of the thermocline circulation as they cross the Cape Basin, with up to 40% of the trapped thermocline water mixed with the environment during the first few months of the eddy’s lifetime. In deeper layers, the tracer content decay may reach up to 90%. Donners et al. (2004) studied the leakage of water from three Agulhas eddies by means of a high-resolution global ocean model using a Lagrangian particle following technique. They found that the dilution of Agulhas eddy water generally increases with depth, with a sharp boundary between particles that stay within the ring and those that mix into the environment; below a depth of 800 m the ring quickly loses its original water mass, and with surface cooling a shallow secondary circulation enhances leakage in the upper 150 m.

Several studies on the subject of the effect of bottom topography on the propagation of Agulhas eddies indicate that the Walvis Ridge may have a significant effect on the propagation of these eddies. Numerical experiments show that the Walvis Ridge affects the amplitude and path of Agulhas eddies; eddies with significant vertical shear can cross the Ridge, but barotropic or near-barotropic eddies cannot (Kamenkovich et al., 1996). Results from an eddy-permitting numerical simulation indicate that most of the anticyclones leave the Cape Basin in a relatively narrow corridor across the Walvis Ridge, with most of the eddy structure confined to the

uppermost levels and with eddy propagation predominantly westward. The cyclones do not leave the basin because they disperse after impinging on the Walvis Ridge, losing their energy to smaller eddies (Matano and Beier, 2003). Altimetric and hydrographic observations provide evidence that the Agulhas eddies cross the Walvis Ridge through its deep gaps where the topographic effect is minimal (Byrne et al., 1995; Schouten et al., 2000).

A recently published collection of papers (Richardson, 2003; Gordon, 2003) describes results of the Indian–Atlantic exchange of water around the Cape of Good Hope into the Cape Basin from field experiments, satellite altimetry and modeling studies. Float trajectories reveal that the Cape Basin is cluttered with anticyclonic and cyclonic eddies, prompting Boebel et al. (2003) to refer the Cape Basin as the Cape Cauldron, a region dominated by turbulent exchange with differential mixing rates throughout the eddy water column. Subsequently, the water trapped within the eddies and that portion blended into the regional background while they reside within the basin contribute to the inter-ocean exchange. Based on the analyses of float and other data, Richardson et al. (2003) proposed a new schematic that illustrates some of the complexity of the exchange in the region (Fig. 1). Intermediate water from the Indian Ocean transported into the South Atlantic by Agulhas eddies, filaments and

blobs appears to be vigorously stirred and mixed with South Atlantic Current Water and also water from the tropical Atlantic by the eddy field. Eventually the blended product of the mixing flows westward across the Walvis Ridge in the Benguela Current and its embedded eddies (Richardson and Garzoli, 2003).

The main objective of this paper simply stated is to determine what the archived hydrographic data tell us about the isopycnal depth variability in the Cape Basin. The Agulhas leakage is a region of intense mesoscale activity and associated isopycnal displacements. There are many publications that detail cruise-specific eddy or ring structures. While these studies may allow for a quantitative analysis of specific eddies, which was the intent of these cruises, the more random distribution of the archived data may expose more of the eddy population characteristics and perhaps a view of the temporal variability. In addition, it allows the determination of the water mass signatures of the thermocline and intermediate layers where significant isopycnal displacements occur with the anticipation of identifying the source of the features. Addressing those goals, in the present study we analyze hydrographic data within the Southeast Atlantic Ocean (10°W–21°E; 20°S–41°S) acquired during the last century along isopycnal surfaces at thermocline levels to develop a view of the

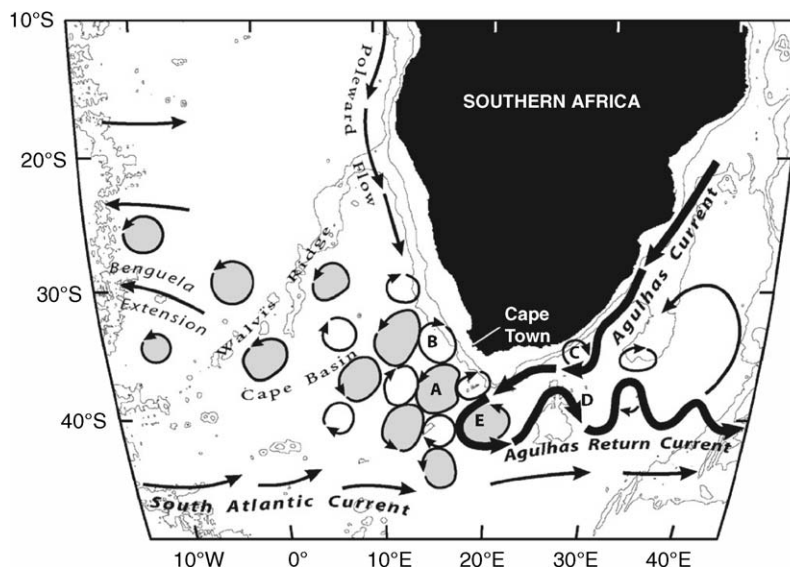


Fig. 1. Schematic map of the circulation of the upper/intermediate layers based on floats trajectories and other recent data (Richardson et al., 2003; Figure 5) with some modifications taken from an earlier schematic by Lutjeharms (1996; Fig. 1). The Cape Basin is populated by numerous anticyclones (A) and cyclones (B). (C) is a cyclonic eddy forming part of a well-developed Natal Pulse on the Agulhas Current. Upstream Retroreflection (D) at the Agulhas Plateau. (E) is the Agulhas Retroreflection.

“climatic” nature of the isopycnal displacements from their long-term mean depths, and to characterize the water masses associated with such isopycnal displacements. Throughout the study, we focus on significant isopycnal displacement features, and for convenience, we refer to these as eddies. The literature suggests that there are varied sources of eddies found within the Cape Basin: those drawn from the Agulhas Retroflection, from the Agulhas cyclonic shear zone falling between southern Africa and the Agulhas Current axis; from the subpolar Atlantic ocean, injected between recently shed Agulhas eddies and the remaining Agulhas Retroflection; and from the Tropical Atlantic introduced to the Cape Basin region along the western margin of Africa (Lutjeharms, 1996; Lutjeharms et al., 2003a; Richardson et al., 2003). It is therefore one of the goals of our study to describe the water-mass properties of eddies found within each of these categories.

2. Data and methods

A vertical section of a typical Agulhas eddy displays the dome-like surface expression of the upper thermocline and the deepening of the isotherms below the surface layer. Two-layer models were successfully applied to describe the upper layer and dynamics of these eddies using the 10 °C isotherm as the interface between the two layers (Olson and Evans, 1986; Olson, 1991; Kamenkovich et al., 1996; Goñi et al., 1997), and several studies used the good correlation between the upper-layer circulation (dynamic height anomaly of the sea surface relative to the 1000 dbar surface) and the depth of the 10 °C isotherm to depict the baroclinic field of the region (Gordon, 1985; Clement and Gordon, 1995; Duncombe Rae et al., 1996; Goñi et al., 1997; Garzoli et al., 1999). Some of these studies also describe and validate the use of altimetry-derived upper layer thickness of the ocean in conjunction with hydrography-derived depth of the 10 °C isotherm to locate Agulhas rings. It should be noted that these regression models between an isotherm and dynamic height perform poorly with the shallowing of the isotherm, suggesting a poor representation of cold cyclonic features (Van Ballegooyen et al., 1994).

Using potential density with respect to the sea surface (σ_0) as a vertical coordinate, we select an isopycnal that would approximately represent the interface between the simple two-layer description

of the density variation with depth. Along the selected isopycnal, depth anomalies computed from the long-term mean are used to identify eddies of the Cape Basin region. With the method and data that we use, we are identifying isopycnal displacements from a long-term mean, not the diameter or shape of the feature; therefore, the use of the term eddy (anticyclonic or cyclonic) provides an accurate depiction of the largest positive or negative isopycnal depth anomalies.

For the present study, we initially assembled a collection of 24,486 hydrographic stations for the period 1901–2002 and for the southeast Atlantic Ocean region within 10°W–21°E and 20°S–41°S. The recent hydrographic data are composed mostly of conductivity-temperature-depth (CTD) measurements, whereas the earlier historical data include bottle data. The data were obtained from the National Oceanographic Data Center (WOD01, Conkright et al., 2002) and from the World Ocean Circulation Experiment (WOCE) Hydrographic Program (WHP) Special Analysis Center (SAC). As the analysis of the data set was based on detection of density anomalies from the long-term mean field by means of basic statistics, first we had to perform a detailed quality control of the extensive data set to identify outliers. Regional potential temperature–salinity diagrams for the thermocline and intermediate waters show a potential density range between 26.5 and 27.5 σ_0 ; thus the first requirement in our quality control procedure was that a station must reach the 27.0 σ_0 surface and have at least three data points between the 26.5 and 27.5 σ_0 range. To avoid including the wind-induced coastal upwelling over the continental shelf (Hardman-Mountford et al., 2003), we excluded those stations with a maximum depth or available bathymetric depth (Smith and Sandwell, 1997) shallower than 600 m. After these initial steps were applied, the original number of hydrographic stations was reduced significantly to less than 4600. Then, all hydrographic data were linearly interpolated to common 10-dbar pressure surfaces. Potential temperature–salinity (θ – S) values from individual stations were compared with the cloud of θ – S from the entire collection, first at all levels, and then using the statistics of the intermediate levels. After several iterative editing procedures our data collection consists of 4145 stations from 1901 to 2002, with only 64 years of data mostly distributed after 1950 (Fig. 2). The horizontal and seasonal coverage provided by the final dataset was fairly

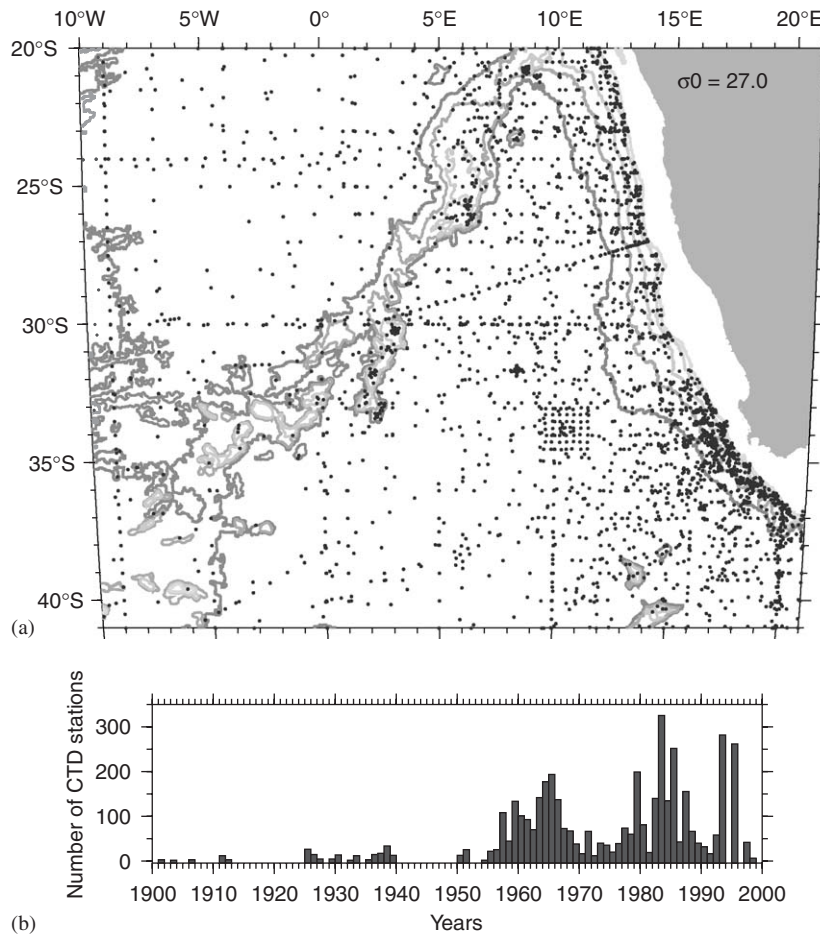


Fig. 2. The station positions (a) and the temporal distribution (b) of the quality controlled dataset along the $\sigma_0 = 27.0$ surface. Bottom topography (Smith and Sandwell, 1997) is delineated by the 600, 1000, 2000, 3000 and 4000 m isobaths. The hydrographic stations were obtained from the combined National Oceanographic Data Center (NODC) and World Ocean Circulation Experiment (WOCE) Hydrographic Program (WHP) databases.

regular over most of the basin with relatively fewer observations west of 2°W. For every 2° latitude by 2° longitude box and with a minimum of four data points (with at least three different seasons represented), monthly and yearly mean and standard deviations were calculated for potential temperature, salinity and pressure along the σ_0 isopycnals between 26.5 and 27.0 (± 0.1 σ -units). For those grid points left blank, we used the gridding method of continuous curvature splines in tension algorithm implemented in the GMT package (Wessel and Smith, 1991; Smith and Wessel, 1990). In this way, for those parameters, we were able to establish climatological mean and standard deviation fields for the period 1901–2002.

The 27.0 (± 0.1 σ -units) σ_0 isopycnal, characteristic of the lower thermocline, was selected as our

reference surface over which anomalies were calculated; maps representing the calculated climatological average pressure, potential temperature and salinity along this isopycnal are shown in Fig. 3. Fig. 3a depicts the large-scale circulation for the regional lower thermocline and upper intermediate levels and resembles for the most part the shape and schematic figure of Peterson and Stramma (1991). The $\sigma_0 = 27.0$ surface lies between 280 and 700 dbar, with a potential temperature range of 6.25–9 °C and a salinity range of 34.35–34.89. It shows deeper values (> 600 dbar) within the subtropical anticyclonic gyre centered near 32°S. The southern and eastern limbs of the gyre can be observed by the shallowing of the isopycnals, lower salinities (< 34.45) and lower potential temperatures (< 7 °C) south of 35°S (South Atlantic Current) but

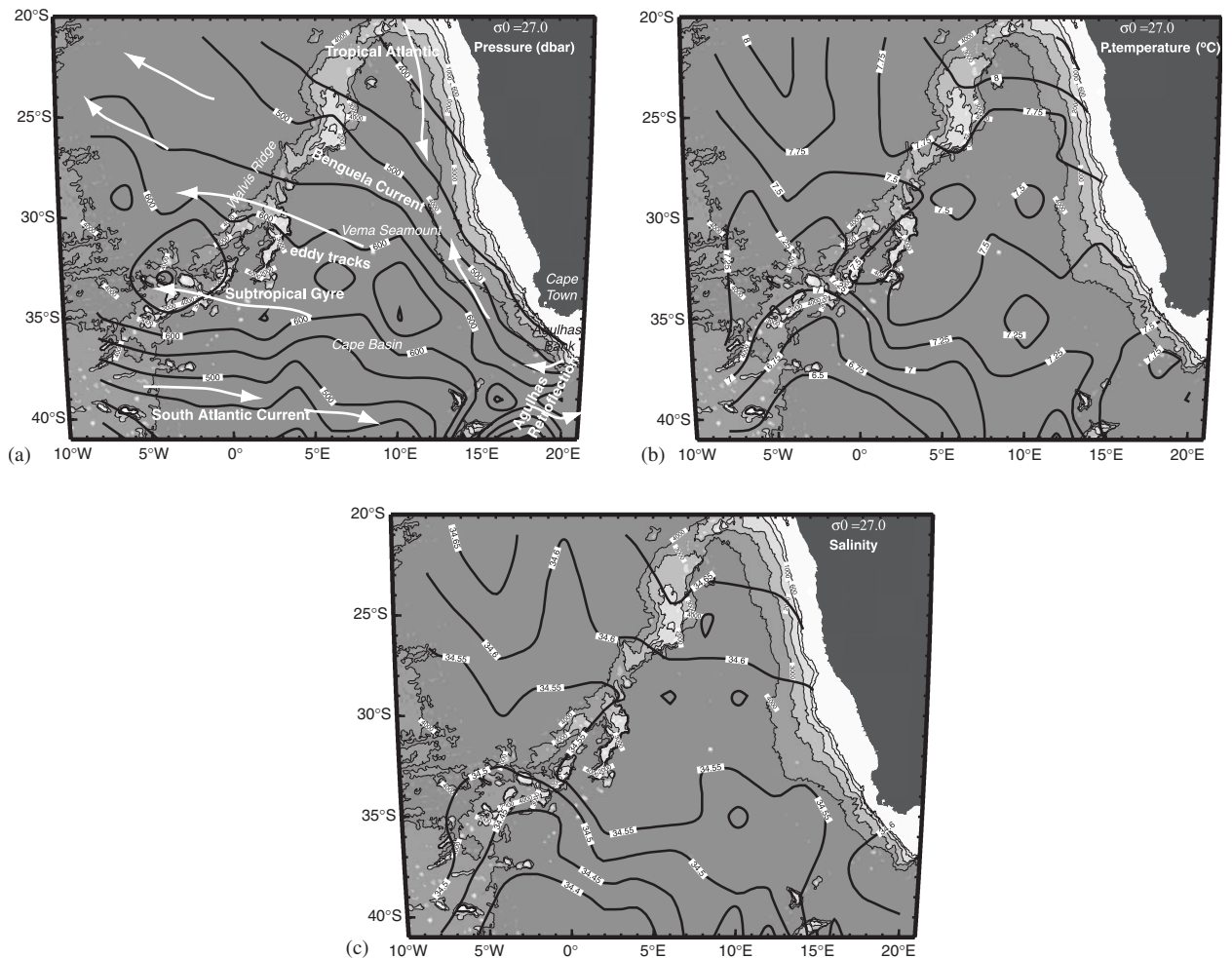


Fig. 3. Maps of the hydrographic climatology pressure (a), potential temperature (b) and salinity (c) fields on the $\sigma_0 = 27.0$ isopycnal surface. The maps are based on the data set shown in Fig. 2a and averaged in 2° latitude/longitude boxes. (a) also includes a schematic circulation at intermediate levels. Isobaths as in Fig. 2. Geographic features labeled in italics.

with higher potential temperatures ($>7.5^\circ\text{C}$) and higher salinities (>34.6) from 15°E to 5°W (Benguela Current). At 37°S , 20°E the loops of the isopleths reveal the Agulhas Retroflexion position, with the turn of the Agulhas Current carrying water back to the Indian Ocean (potential temperatures $>7.7^\circ\text{C}$ and salinities >34.6). North of 25°S along 10°E approximately, higher temperatures ($>8^\circ\text{C}$) and salinities (>34.65) reflect the Atlantic water of tropical origin. The isopleths in the central region portray the highly variable nature of the region with ring patterns and the water contributions of different origins, with higher temperatures and salinities associated with the Indian Ocean and lower temperatures and salinities from South Atlantic water masses.

As mentioned above, to identify eddies we compare the depth of the $27.0 (\pm 0.1 \sigma\text{-units}) \sigma_0$ isopycnal, hereafter-denoted zS27, for each individual station with the climatological mean and standard deviation (SD) value estimated for every 2° box, to detect the vertical displacements of this particular isopycnal and thus the presence of anticyclonic (deeper) or cyclonic (shallower) eddies. To avoid spatial or temporal aliasing introduced by a particular cruise, we averaged the data for the same cruise in each grid box. The resultant zS27 anomalies were grouped by SD intervals (0 to ± 1 ; ± 1 to 2 and ± 2). The normal probability plot of the zS27 values (not included) correspond to the straight line representing the reference normal distribution within approximately, -4 to 4 SD;

beyond those limits, the data depart from the straight line. The histogram of zS27 anomalies is given in Fig. 4; it displays an approximately normal distribution with a median value of 0.0284 and a standard deviation of 1.1344.

To quantify the water masses carried by eddies at upper/intermediate levels, we measured their salinity differences along σ_0 surfaces, relative to three major source water masses for the region. At the depths of interest, the selected sources represent the Atlantic contribution of Antarctic Intermediate Water (AAIW), the South Indian Ocean component of intermediate waters (Red Sea Water), and tropical thermocline waters of the South Atlantic. The 26.5 ($\pm 0.05 \sigma$ -units) and 27.0 ($\pm 0.05 \sigma$ -units) σ_0 surfaces were chosen for the upper thermocline and lower thermocline/upper intermediate, respectively. Along those surfaces, salinity differences were calculated relative to a mean reference salinity value, in this case the Agulhas Current, and to the other two source water masses, South Atlantic Current (SAC) and Tropical Atlantic Water. Thus, scaling the differences relative to the three sources, but using the Agulhas Current mean value as our reference value, eddies will carry Agulhas Water if their salinity anomalies will fall within ± 5 units of the mean reference value. For example, for a particular eddy we calculate a mean salinity (S) along one of the chosen isopycnals. Its salinity S is compared to the mean salinity values from the source water masses along the same isopycnal. If in this particular case, S falls between the mean South Atlantic Current salinity value (S_{SAC}) and the mean Agulhas Current salinity value (S_{AC}), calculated along the same isopycnal, then we define the salinity anomaly as

$$\delta S = 10 * (S - S_{AC}) / (S_{AC} - S_{SAC}).$$

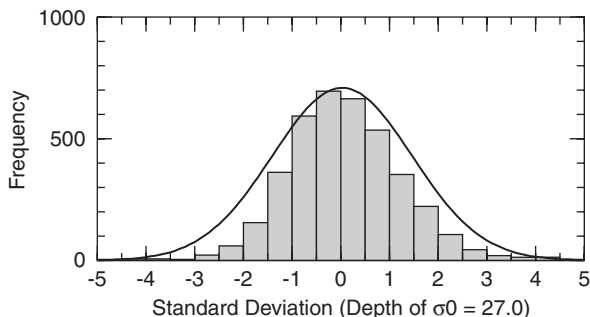


Fig. 4. Histogram of the $\sigma_0 = 27.0$ isopycnal depth anomalies relative to the long-term mean for the entire period. Overlapped in the same diagram is the normal distribution fit for the histogram.

3. Results

3.1. Eddy distribution

The comparison of the zS27 for each hydrographic data point with the calculated climatological mean allows us to produce a map of the isopycnal displacements in the basin. In Fig. 5, we display the distribution of all the isopycnal depth anomalies beyond 1 and 2 SD and averaged into 2° boxes. The 1SD results are distributed uniformly throughout the basin with approximately an equal number of negative and positive isopycnal displacements. The reduced data set from the 2SD results is distributed mainly on the eastern side of the basin (east of 0°). We attribute the larger of these displacements, represented by 2SD results, to the energetic eddies characteristic of the Cape Basin: shallowing are cyclonic eddies, deepening are representative of anticyclonic eddies. These larger displacements indicate that there is a 2:1 anticyclone/cyclone ratio. Lesser displacements [1SD], of the less energetic features, are almost evenly split between anticyclonic and cyclonic eddies with a ratio of 1.4:1. The percentages of anticyclones and cyclones for the larger displacements and only for those grid cells with at least four different seasons are presented in Figs. 6a and b. Within the region, we find distinct isopycnal displacements. In the $25\text{--}40^\circ\text{S}$ latitudinal band (Fig. 6a), the distribution of the positive displacements within the 5–15% range towards the north and west is consistent with the distribution of anticyclones that have been observed with floats and altimetry (Boebel et al., 2003) and with historical hydrographic observations analyzed together with altimetry (Van Veldhoven, 2005, Figure 5.1). The cyclones (Fig. 6b) display a more localized distribution with lower percentages (5%) within the Cape Cauldron and higher values (20%) at approximately 25°S , east of the Walvis Ridge. The percentages, and the ratio, of anticyclones and cyclones between the latitudes of 20 and 37°S and every 2° of longitude, or latitude, are plotted in Figs. 6c and d. From Figs. 6c and d, and other eddy distributions not shown, we find higher percentages of anticyclones and ratios on the eastern side of the basin, east of 10°E and south of 30°S . The anticyclones show higher percentages with higher ratios at 20°E , mostly due to the higher number of anticyclones at the Retroflexion, and at 14°E due to a higher number of anticyclones south of 30°S . The lower ratio at 18°E is attributed to a

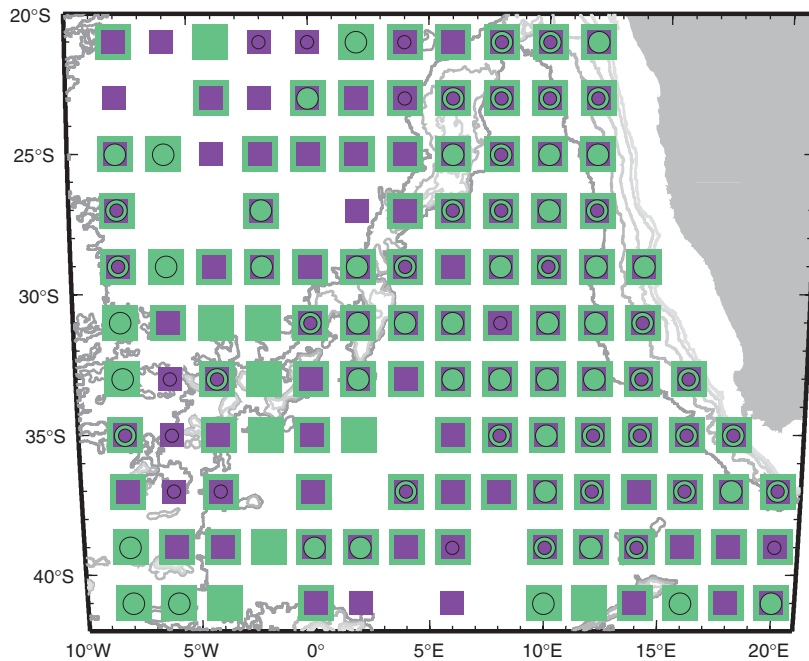


Fig. 5. Distribution of the $\sigma_0 = 27.0$ isopycnal depth anomalies relative to the long-term mean field averaged on 2° latitude/longitude boxes. Colors represent the positive (green) or negative (purple) anomalies and the symbols the number of standard deviations ($>1SD$, squares; $>2SD$, circles).

higher number of cyclones, mostly in the Cape Cauldron region. Between the longitudes of 10 and $8^\circ E$, the ratio decreases because of the higher number of cyclones, contributed mainly from latitudes north of $29^\circ S$. Most of the cyclones tracked by Richardson and Garzoli (2003) using floats translated southwestward in the Cape Basin, but they also tracked a cyclone north of $30^\circ S$, probably generated by intense Agulhas rings that became unstable and broke into pieces near Vema Seamount ($31.7^\circ S$, $8.4^\circ E$). They observed floats in two cyclones, which looped near Vema Seamount, where numerous rings have been observed by satellite to bifurcate (Schouten et al., 2000). Between 6 and $4^\circ E$, in the vicinity of the Walvis Ridge, the higher percentages of anticyclones are found between 31 and $33^\circ S$, with the cyclones distributed mostly north of $27^\circ S$. At 0° , a high, but almost equal, number of features are found at $31^\circ S$. The distribution of the ratios is located practically within the schematic “Agulhas eddy corridor” described by Garzoli and Gordon (1996), and it agrees with other ring distributions based on float trajectories presented by Richardson and Garzoli (2003). The Cape Basin is a highly energetic region, where eddies can interact with other eddies, split,

and merge (Boebel et al., 2003; Schouten et al., 2000), making the tracking of these features as they move through the basin very difficult. Consequently, we find a wide range of lifetime estimates. Boebel et al. (2003) report that within the Cape Basin the majority of anticyclones have lifetimes of around 100 days, with 60–90 days for cyclones; Richardson and Garzoli (2003) with floats and altimetry could track eddies for up to 27–30 months. Once outside this region, eddies can penetrate the South Atlantic subtropical gyre, where they can persist more than 2 years (Byrne et al., 1995) with a more coherent structure. Based on the above estimates, it is entirely possible that we are counting the same eddy more than once, but at various stages of its lifetime; it is also likely that the eddy will be located in a different grid box. To minimize these possible temporal/spatial biases, on any particular grid-box the same cruise measurements were combined and all seasons were treated equally.

3.2. Origin of the thermocline water within the eddies

As described previously, in order to determine the water mass composition and origin of the zS27 anomaly-based features, we selected three sets of

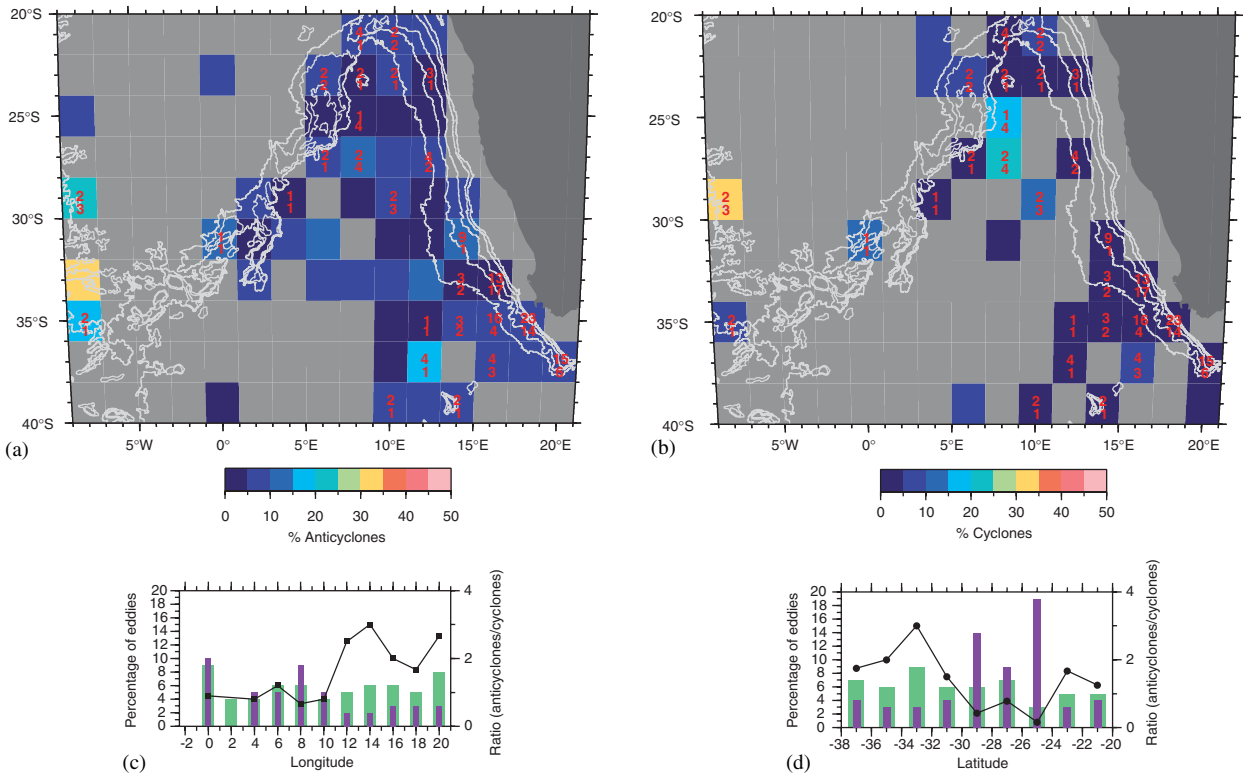


Fig. 6. Percentage of anticyclones (a) and cyclones (b) in each 2° latitude/longitude box for the largest $\sigma_0 = 27.0$ isopycnal depth anomalies ($>2SD$) and for those grid boxes with at least four different seasons. The numbers in red represent the number of anticyclones and cyclones in each grid box. (c) and (d) Distribution of the percentage of eddies (green and purple bars) and the ratio (anticyclone/cyclone; solid black line) vs. longitude and latitude, respectively. The original 2° latitude/longitude eddy distribution was averaged from 20 to $37^\circ S$ and displayed every 2° in longitude or latitude.

stations representing the main source water masses for this region. Salinity and oxygen data against potential temperature, along with the geographic locations for those reference stations, are shown in Fig. 7.

The $\theta-S$ and $\theta-O_2$ relationships for those stations with $zS27$ anomalies beyond $2SD$ are also plotted in Fig. 7. Following earlier water mass composition descriptions for this region (Valentine et al., 1993; Gordon et al., 1987), we identified Subtropical Surface Water and Subantarctic Surface Waters, Central or Thermocline Water (Atlantic and Indian), AAIW and Red Sea intermediate water (Beal et al., 2000), and below, the deep waters, with NADW, Circumpolar Deep Water (CDW), and Antarctic Bottom Water (AABW).

3.2.1. Low oxygen content at thermocline levels

The $\theta-O_2$ diagram (Fig. 7b) shows a range of low oxygen values, below 4 ml/l , for temperatures within $6-15^\circ C$. θ and S vertical profiles, $\theta-S$ and $\theta-O_2$

diagrams for the stations with this characteristic low oxygen at thermocline levels, and for the reference stations, are displayed in Fig. 8. Within this group, we found an approximately equal number of cyclones and anticyclones, distributed in the northern and southeastern Cape Basin. Within the southeast area, south of $33^\circ S$, cyclones seem to be confined mostly between the African margin and the 3000 m isobath, with anticyclones identified further offshore, between the 3000 and 4000 m isobaths. The anticyclones show surface waters with Agulhas Current characteristics, with a temperature range of $16-24^\circ C$ and salinities for the most part between 35.4 and 35.5 ; in comparison the cyclones display both lower surface temperature (maxima $22^\circ C$) and salinities ($35.2-35.5$). The thermocline levels display temperature and salinity properties between those of the SAC and Agulhas Current and with oxygen values between 3.5 and 4 ml/l . $\theta-S$ and $\theta-O_2$ properties for both anticyclones and cyclones at intermediate depths, show a reduced RSW effect in

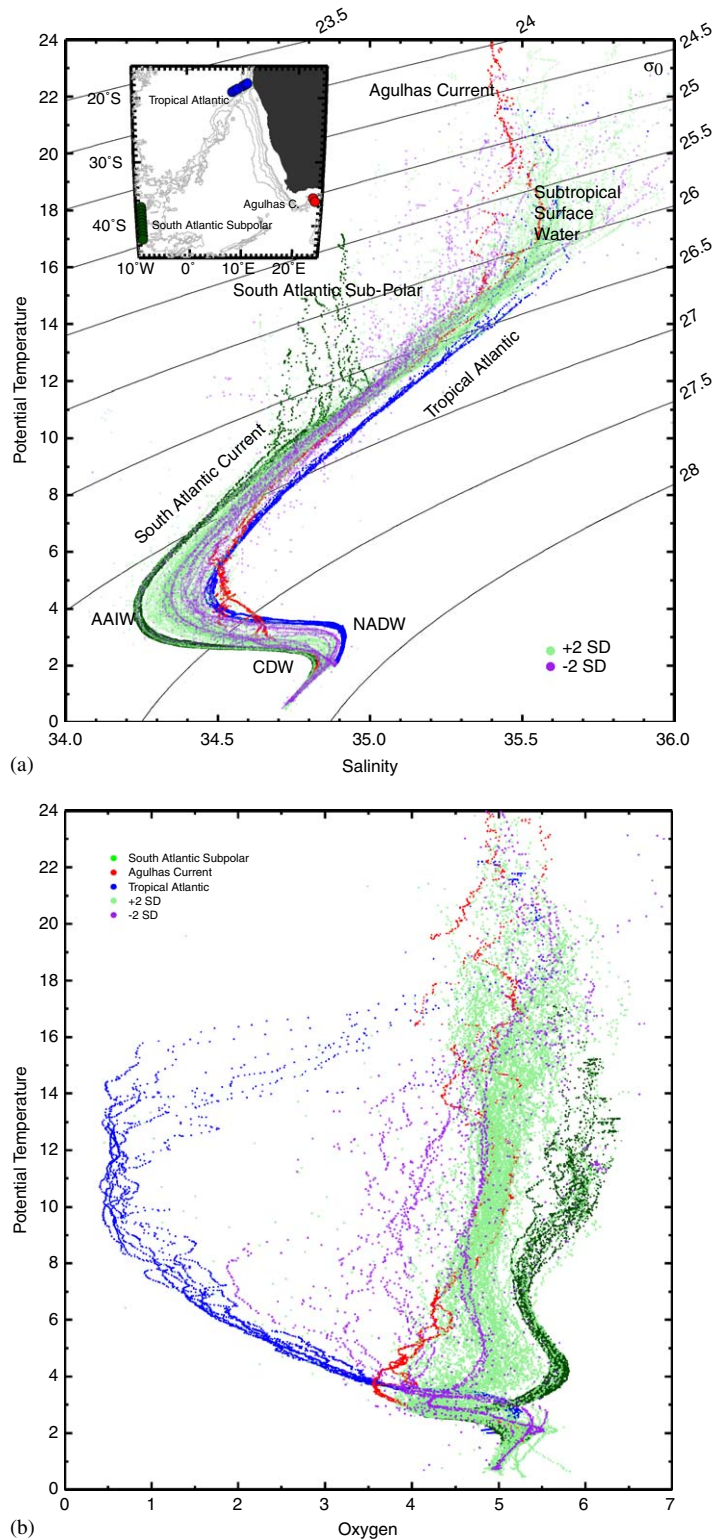


Fig. 7. Potential temperature versus salinity (a) and potential temperature versus oxygen (b) characteristics for those stations where the $27.0\sigma_0$ isopycnal depth anomalies are deeper (light green; $>2SD$) or shallower (purple; $<-2SD$) than the mean field. Contours are lines of constant potential density referenced to 1000 dbar and are drawn every $0.1\sigma_0$ -units. Dark green represents stations for South Atlantic Current (WOCE A14, stations: 90–100), blue indicates Tropical Atlantic Water (WOCE A09, stations: 226–232) and red represents Agulhas Current (Agulhas Retroflection Cruise ARC, stations: 49–50). See the inset for station positions. These stations will represent the main source of water masses in our study region.

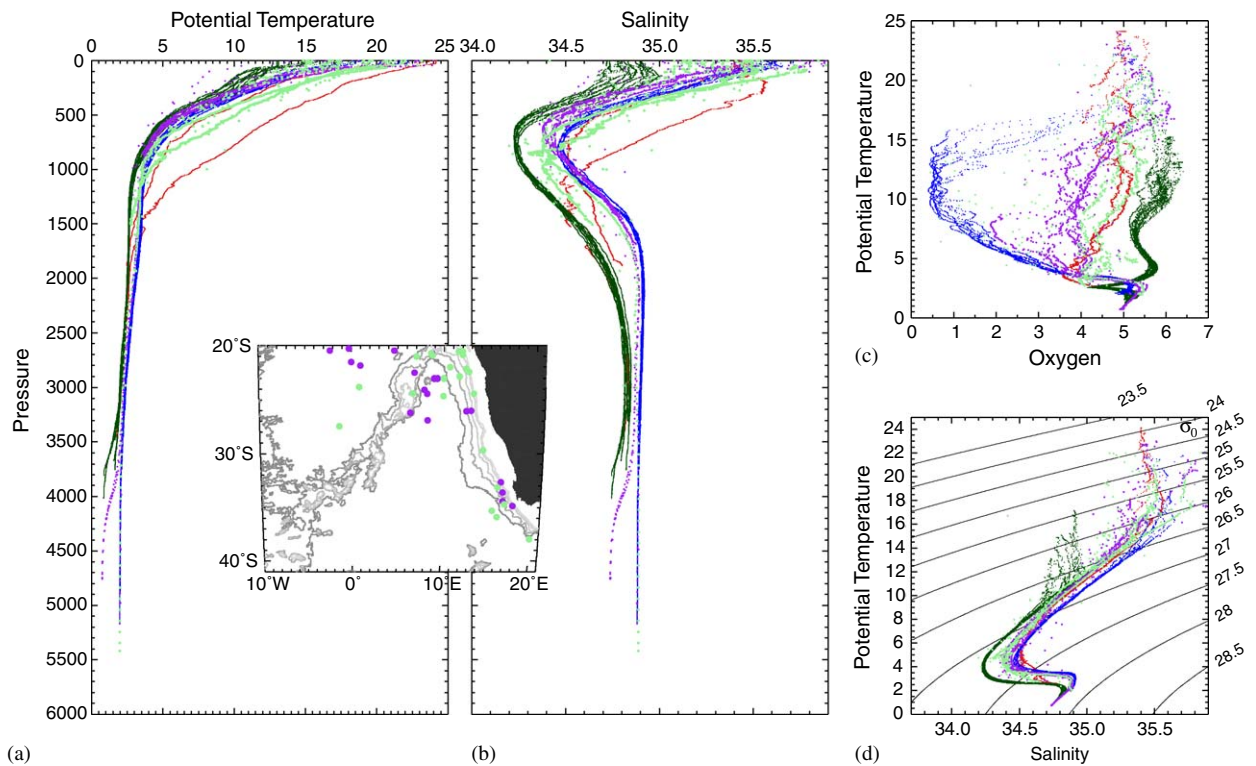


Fig. 8. Potential temperature (a) and salinity (b) profiles, potential temperature versus oxygen (c) and versus salinity (d) for stations with low oxygen content, below 4 ml/l, for potential temperatures within 6–15 °C and for the selected three water mass sources for the region (in red, Agulhas Current; blue, Tropical Atlantic; and dark green, South Atlantic Current). Light green corresponds to anticyclones and purple to cyclones. Also shown in the inset, the location of these stations.

the Agulhas Current by interleaving with AAIW waters suggesting lateral mixing between these contrasting water masses; consequently, we observe a freshening and higher oxygenation at these depths, with salinities lower than 34.4 and oxygen values up to 5 ml/l. Schmid et al. (2003) found various examples of vigorous exchange between rings and its surroundings at intermediate depths, with interleaving of water parcels with different hydrographic properties leading to enhanced mixing.

In the northern part of the basin, there is a more widespread distribution, with an increased number of cyclones west of 10°E, closer to the Walvis Ridge (Fig. 8, map). Eddies found between this longitude and the African coast seem to be Agulhas water modified by oxygen consumption by biological processes within the Benguela upwelling region (Gordon et al., 1992, 1995; Gordon and Bosley, 1991). At the surface, the θ - S and θ - O_2 diagrams for temperatures above 14 °C, display salinities between 35.2 and 35.4 and oxygen values between 4.5 and 5.5 ml/l; at thermocline levels, we observe

water properties similar to those of the Agulhas Current. The profiles for cyclones identified west of 10°E have mid-depth characteristics that resemble those of the Tropical Atlantic Water with oxygen values lower than 4.0 ml/l; we observe one profile, corresponding to an anticyclone, located west of the Walvis Ridge with Tropical Atlantic Water at deep levels. Richardson and Garzoli (2003) observed this low-oxygen Tropical South Atlantic Water in this same area with floats that drifted southward, supporting the conclusion that low-oxygen, higher-salinity tropical water is being advected southward in the Cape Basin.

3.2.2. High oxygen content at intermediate layers

Temperature, salinity and oxygen data are plotted for eddies with high oxygen content in the AAIW layer (salinity < 34.4, oxygen > 5.25 ml/l and temperature 3–5 °C; Figs. 7b and 9). The majority of eddies found with these characteristics have anticyclonic rotation (80%) and they are observed mainly in the southern part of the basin, south of

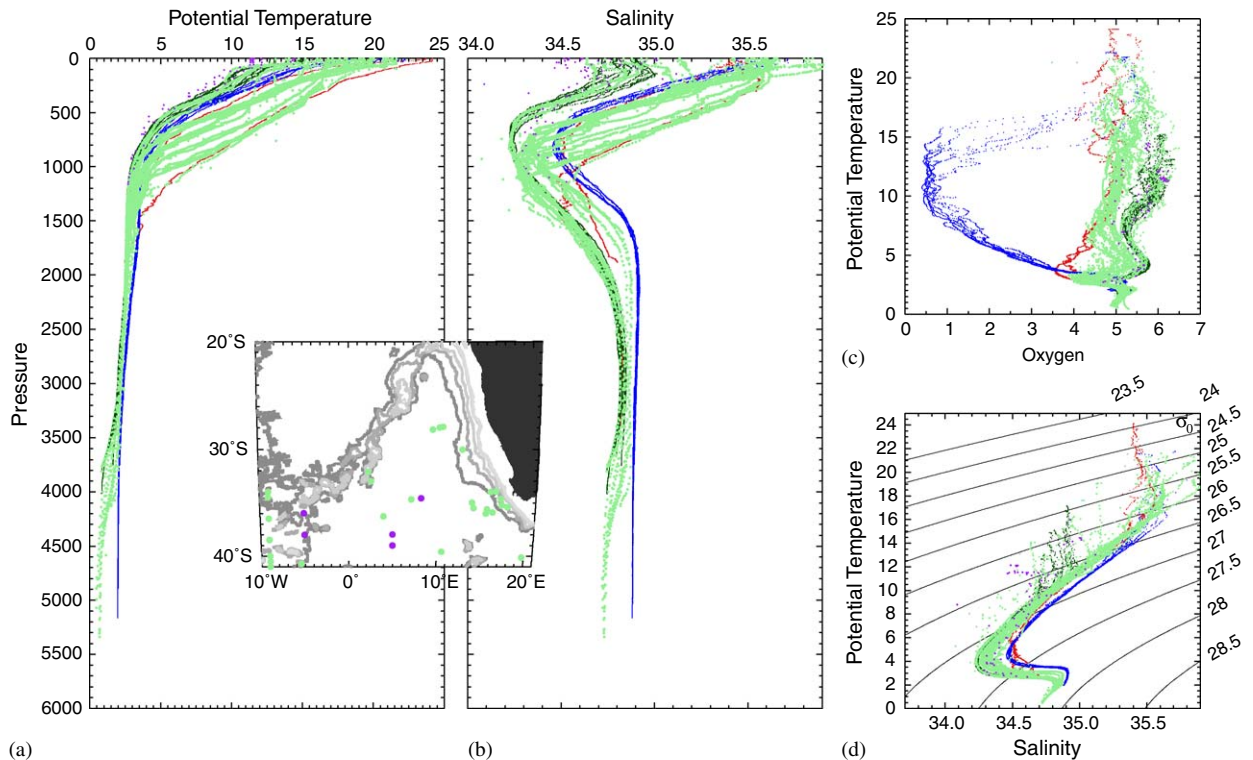


Fig. 9. Same as Fig. 8, except for those stations with high oxygen content at intermediate levels (salinity < 34.4, oxygen > 5.25 ml/l, and potential temperature 3–5 °C).

30°S. Most of the anticyclones are identified in the southeastern Cape Basin and west of the Walvis Ridge, whereas the cyclones are located in the southern central Cape Basin, between the longitudes of 5°W and 10°E. These cyclones contain concentrated AAIW of subantarctic origin at intermediate levels. However, we also see a small number of anticyclones sharing this same characteristic; these are located west of the Walvis Ridge, south of 35°S, mainly between 10 and 5°W. As we approach the margin of the African continent, there is evidence of mixing at intermediate depths due to subantarctic water slipping under the Agulhas thermocline water. The anticyclones identified at the latitude of Cape Town, with surface salinities higher than the Agulhas Current value and increased oxygen concentrations, may be a product of convective modification (Olson et al., 1992).

3.2.3. Salinity anomalies at thermocline/intermediate levels

θ - S properties (Fig. 7a) along the $\sigma_0 = 26.5$ isopycnal for those eddies identified as cyclones reveal negative salinity and temperature anomalies

with respect to an Agulhas Current mean value of approximately 0.1 and 0.5 °C, respectively. In the lower thermocline, along the 27.0 σ_0 surface, most of the data points fall between the SAC and Agulhas Current water curves. At intermediate depths, the data profiles show a range of salinities distributed mostly towards the Agulhas Current maximum and, in some profiles, even Tropical Atlantic Water.

For the upper thermocline, the anticyclones display both positive and negative salinity anomalies, within 0.1 of the mean Agulhas Current value at that level. At the lower thermocline and intermediate levels, data points are distributed throughout the entire θ - S space between the Agulhas Current and SAC sources, although with a stronger presence of subantarctic water.

As described above, to quantify the water masses carried by eddies in the upper and lower thermocline/upper intermediate levels, we calculate their salinity differences along σ_0 surfaces, relative to the three major sources selected for the region. We choose the 26.5 σ_0 surface for the upper thermocline and a $\sigma_0 = 27.0$ surface for the lower thermocline.

Maps of the isopycnal salinity differences, for both anticyclones and cyclones, are plotted in Figs. 10a–d. These maps in part summarize the results previously discussed. Fig. 10a indicates that most of the anticyclones carry Agulhas Current water at thermocline levels, with positive salinity anomalies in the Retroflexion and Cape Cauldron areas, most likely products of local atmospheric cooling (Gordon et al., 1987). Negative salinity anomalies confined mainly south of approximately 37°S and west of 5°E, associated with the SAC,

bringing fresh AAIW from the western South Atlantic into the southern Cape Basin. The cyclones (Fig. 10b) carrying SAC dominate the region south of 37°S, with more concentrated SAC values in the southwest of the basin and with values closer to our Agulhas Current mean value in the Cape Cauldron. Agulhas Current cyclones, slightly fresher, are seen between the Agulhas Current axis and the African margin.

On those maps representing the lower thermo-
cline/upper intermediate layer, we also plotted those

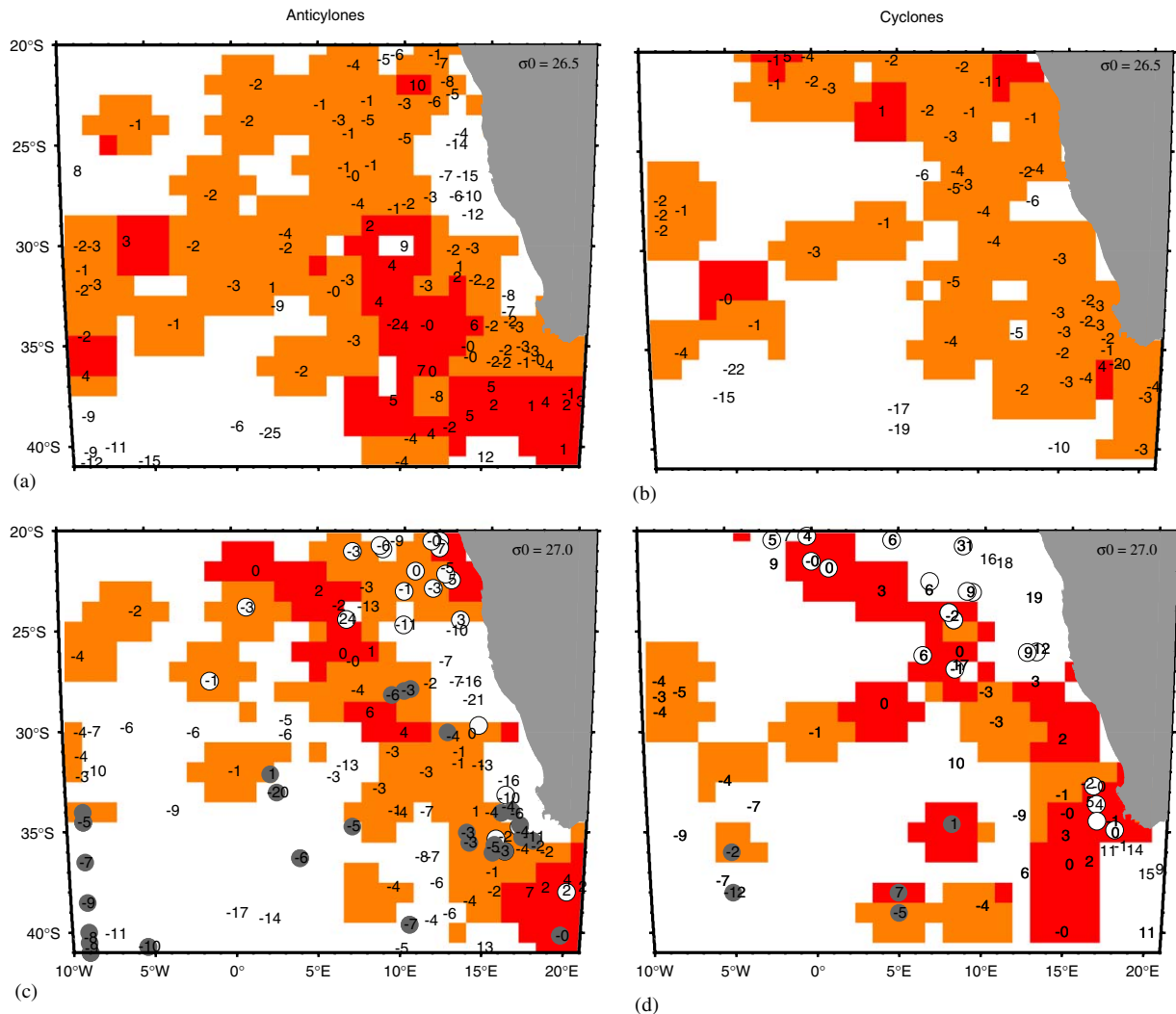


Fig. 10. Upper panels: salinity anomalies on the $\sigma_0 = 26.5$ surface; anticyclones (a) and cyclones (b); in the lower panels, same as in the upper panels, except for $\sigma_0 = 27.0$ (lower thermocline); anticyclones (c) and cyclones (d). The numbers represent the salinity differences that were calculated along the $\sigma_0 = 26.5$ and 27.0 isopycnals and relative to a mean reference salinity value, in this case the Agulhas Current, and to the other two source water masses, South Atlantic Current and Tropical Atlantic. Colored areas correspond to salinity differences within ± 5 units from the Agulhas Current mean value at each isopycnal level (0 to 5 red; -5 to 0 orange). Also plotted, those stations with low (open circles; see also Fig. 8) and high (gray solid circles, see also Fig. 9) oxygen content at thermocline/intermediate levels.

stations with low and high oxygen content described in Sections 3.2.1 and 3.2.2 (also, Figs. 8 and 9). The anticyclonic field (Fig. 10c) shows a narrower northwest distribution of Agulhas Current water, whereas within the southwestern part of the basin the negative salinity anomalies and higher oxygen values shows stronger mixing with SAC at these levels. Increased oxygen concentrations found for those stations west of Cape Town are the product of local thermohaline modifications by sea-air fluxes on the Agulhas water (Gordon et al., 1987; Olson et al., 1992). Positive salinity anomalies and low oxygen content values for cyclones north of 25°S (Fig. 10d) are indications of Tropical Atlantic Water influence. Figs. 7 and 10 (and other vertical profiles not shown) reveal that cyclonic and anticyclonic eddies are composed of Agulhas Current thermocline water, somewhat enriched in AAIW properties directly from the Atlantic subpolar as these waters slip under the Agulhas thermocline water. The thermocline level is dominated by anticyclonic Agulhas eddies derived from the Agulhas Retroflection, with a northwestern distribution resembling the “Agulhas Eddy Corridor”; the cyclones have a narrower distribution and are likely to be shear eddies generated between the Agulhas Current axis and the southern rim of Africa (Lutjeharms et al., 1989; Lutjeharms et al., 2003a, b).

At intermediate levels, the anticyclones have θ - S properties closer to those of the South Atlantic Central Water, indicating a stronger interaction with this water mass at these depths, consequently with lower salinities and higher oxygen values and with a narrower distribution of anticyclones carrying Agulhas Current properties. In contrast, cyclones show positive salinity anomalies close the African margin and with a southwestward distribution between 5 and 10°E. These distributions suggest that cyclones have θ - S characteristics closer or less diluted to those of the Agulhas Current waters at this level.

4. Summary and conclusions

Mesoscale activity and related isopycnal displacements associated with the Agulhas leakage in the Cape Basin region is intense. There are many publications that detail cruise specific eddy structures for the region. While these studies may allow for a quantitative view of specific eddies, which was the intent of these cruises, the more random distribution of the archived data may expose more

of the eddy population characteristics. Therefore, our main objective simply stated was to determine what the archived hydrographic data could tell us about isopycnal depth variability in the Cape Basin. An additional objective was to determine the water mass signatures of the thermocline and intermediate layers which are linked to significant isopycnal displacements, with the anticipation of identifying the source of the feature.

In the present study, with the nearly century long record of hydrographic stations within the Cape Basin region of the southeast Atlantic Ocean, methods were developed to identify isopycnal displacements from the long-term mean depth of the 27.0 σ_0 isopycnal. The sampling methods used, described in the text, and in course of this investigation greatly minimized temporal and spatial sampling biases. We attributed the larger of the isopycnal displacements, represented by 2 standard deviations (SD), to the energetic eddies characteristic of the Cape Basin: shallowing are cyclonic eddies, deepening are representative of anticyclonic eddies. Numerous eddies were identified in the whole region. The larger displacements indicate that there is a 2:1 anticyclone/cyclone ratio. Lesser displacements of the less energetic features, captured by the 1 SD field, are almost equally split between anticyclones and cyclones (1.4:1 ratio). The more energetic features are found in the region approximately within 12–20°E and 33–39°S (Cape Cauldron). Within this area, the cyclones seem to be more geographically confined with a southwestward distribution, whereas anticyclones show a northwest dispersal. Not all cyclonic eddies are purely subantarctic water, but rather appear to be Agulhas thermocline water. The lower temperatures and salinities found in some cyclones are possibly related to their origin in the shear zone between the Agulhas Current axis and Africa (Lutjeharms et al., 1989). Along the continental shelf-edge, these intense shear eddies, driven by the passing Agulhas Current upwell cold, dense, South West Indian Central Water in their cores (Lutjeharms et al., 2000). In addition, the anticyclonic eddies, while normally composed of Agulhas water, often contain fairly pure Antarctic Intermediate Water (AAIW), suggesting subduction of Atlantic subpolar water; along the northern region of the study area they incorporate the low-oxygen thermocline from the Tropical Atlantic Ocean.

The θ - S relationship within the anticyclonic eddies is mainly of Agulhas water properties for

surface and thermocline waters. At intermediate levels, the range of θ - S values between the saline Red Sea Water (RSW) and the fresher AAIW indicates strong stirring of Indian and Atlantic waters at these depths.

On proceeding northward along the western margin of the African continent, both cyclones and anticyclones incorporate increasing amounts of Tropical Atlantic water, which enters the region with a poleward flowing undercurrent over the slope. Only cyclones along approximately 10°E and north of 25°S show almost pure Tropical Atlantic characteristics, with low-oxygen thermocline values and a weakened AAIW influence. West of the Walvis Ridge, there is no indication of subantarctic water signature at depth, but pure Tropical Atlantic water instead. It is south of 30°S, crossing the Walvis Ridge, where we observe much clearer subantarctic water characteristics.

Our analysis implies that at thermocline and intermediate levels, both anticyclones and cyclones of the Cape Basin play a significant role in the Agulhas leakage. The eddy core water is not solely drawn from the Indian Ocean: tropical and subtropical Atlantic water are also present; The results also indicate that distinct water masses are mixed differently throughout the water column of the eddy and in different regions of the basin. These conclusions are consistent with other recent studies based on floats and altimetry (Boebel et al., 2003; Richardson and Garzoli, 2003).

Various questions remain unanswered and are mainly related to the temporal variability of the isopycnal displacements. With the present data set, we were not able to extract a clear signal, but in future work we propose to include other data sets and to enlarge the area of study in order to address those questions.

Acknowledgments

This research was funded in full under the Cooperative Institute for Climate Applications and Research (CICAR) award number NA03OAR4320179 from the National Oceanic and Atmospheric Administration, US Department of Commerce. The statements, findings, conclusions, and recommendations are those of the authors and do not necessarily reflect the views of the National Oceanic and Atmospheric Administration or the Department of Commerce. We thank the reviewers and editor for their valuable com-

ments, Deirdre Byrne for useful suggestions, Phil Mele for providing and maintaining the data archive, and Martin Fleisher for his careful comments on the manuscript. LDEO contribution number 6915.

References

- Beal, L.M., Field, A., Gordon, A.L., 2000. Spreading of Red Sea overflow water in the Indian Ocean. *Journal of Geophysical Research Oceans* 105 (C4), 8549–8564.
- Byrne, D.A., Gordon, A.L., Haxby, W.F., 1995. Agulhas Eddies: a synoptic view using GEOSAT ERM data. *Journal of Physical Oceanography* 25, 902–917.
- Boebel, O., Lutjeharms, J.R.E., Schmid, C., Zenk, W., Rossby, H.T., Barron, C., 2003. The Cape Cauldron: a regime of turbulent inter-ocean exchange. *Deep-Sea Research Part II* 50, 57–86.
- Clement, A.C., Gordon, A.L., 1995. The absolute velocity field of Agulhas eddies and the Benguela current. *Journal of Geophysical Research—Oceans* 100 (C11), 22591–22601.
- Conkright, M.E., Antonov, J.I., Baranova, O., Boyer, T.P., Garcia, H.E., Gelfeld, R., Johnson, D., Locarnini, R.A., Murphy, P.P., O'Brien, T.D., Smolyar, I., Stephens, C., 2002. *World Ocean Database 2001, Volume 1: Introduction*. In: Levitus, S. (Ed.), NOAA Atlas NESDIS 42, US Government Printing Office, Washington, DC, 167pp.
- de Ruijter, W.P.M., Biastoch, A., Drijfhout, S.S., Lutjeharms, J.R.E., Matano, R.P., Pichevin, T., van Leeuwen, P.J., Weijer, W., 1999. Indian–Atlantic interocean exchange: dynamics, estimation and impact. *Journal of Geophysical Research* 104 (C9), 20,885–20,910.
- de Steur, L., van Leeuwen, P.J., Drijfhout, S.S., 2004. Tracer leakage from modeled Agulhas rings. *Journal of Physical Oceanography* 34 (6), 1387–1399.
- Donners, J., Drijfhout, S.S., Coward, A.C., 2004. Impact of cooling on the water mass exchange of Agulhas rings in a high resolution ocean model. *Geophysical Research Letters* 31 (16) Art. no. L16312.
- Duncombe Rae, C.M., 1991. Agulhas Retroflexion rings in the South Atlantic Ocean; an overview. *South African Journal of Marine Science* 11, 327–344.
- Duncombe Rae, C.M., Garzoli, S.L., Gordon, A.L., 1996. The eddy field of the southeast Atlantic Ocean: a statistical census from the Benguela sources and transports project. *Journal of Geophysical Research* 101, 11949–11964.
- Flierl, G.R., 1981. Particle motions in large-amplitude wave fields. *Geophysical and Astrophysical Fluid Dynamics* 18 (1–2), 39–74.
- Garzoli, S.L., Gordon, A.L., 1996. Origins and variability of the Benguela Current. *Journal of Geophysical Research* 101, 897–906.
- Garzoli, S.L., Richardson, P.L., Duncombe Rae, C.M., Fratantoni, D.M., Goñi, G.J., Roubicek, A.J., 1999. Three Agulhas Rings observed during the Benguela Current experiment. *Journal of Geophysical Research* 104 (C9), 20971–20986.
- Goñi, G.J., Garzoli, S.L., Roubicek, A.J., Olson, D.B., Brown, O.B., 1997. Agulhas ring dynamics from TOPEX/POSEIDON satellite altimeter data. *Journal of Marine Research* 55, 861–883.

- Gordon, A.L., 1985. Indian–Atlantic transfer of thermocline water at the Agulhas Retroflection. *Science* 227, 1030–1033.
- Gordon, A.L., 1986. Inter-ocean exchange of thermocline water. *Journal of Geophysical Research* 91 (C4), 5037–5046.
- Gordon, A.L., 1996. Communication between oceans. *Nature* 382 (6590), 399–400.
- Gordon, A.L., 2003. Oceanography—the brawniest Retroflection. *Nature* 421 (6926), 904–905.
- Gordon, A.L., Bosley, K.T., 1991. Cyclonic gyre in the tropical South-Atlantic. *Deep-Sea Research Part A—Oceanographic Research Papers* 38, S323–S343.
- Gordon, A.L., Lutjeharms, J.R.E., Gründlingh, M.L., 1987. Stratification and circulation at the Agulhas Retroflection. *Deep-Sea Research* 34A (4), 565–599.
- Gordon, A.L., Weiss, R.F., Smethie Jr., W.M., Warner, M.J., 1992. Thermocline and intermediate water communication between the south Atlantic and Indian Oceans. *Journal of Geophysical Research* 97 (C5), 7223–7240.
- Gordon, A.L., Bosley, K.T., Aikman, F., 1995. Tropical Atlantic Water within the Benguela upwelling system at 27°S. *Deep-Sea Research Part I* 42 (1), 1–12.
- Gordon, A.L., Barnier, B., Speer, K., Stramma, L., 1999. World Ocean Circulation Experiment: South Atlantic results. *Journal of Geophysical Research* 104 (C9), 20859–20861.
- Hardman-Mountford, N.J., Richardson, A.J., Agenbag, J.J., Hagen, E., Nykjaer, L., Shillington, F.A., Villacastin, C., 2003. Ocean climate of the South East Atlantic observed from satellite data and wind models. *Progress in Oceanography* 59 (2–3), 181–221.
- Kamenkovich, V.M., Leonov, Y.P., Nechaev, D.A., Byrne, D.A., Gordon, A.L., 1996. On the influence of bottom topography on the Agulhas eddy. *Journal of Physical Oceanography* 26 (6), 892–912.
- Lutjeharms, J.R.E., 1996. The exchange of water between the South Indian and South Atlantic Oceans. In: Wefer, G., Berger, W.H., Siedler, G., Webb, D. (Eds.), *The South Atlantic: Present and Past Circulation*. Springer, Berlin–Heidelberg, pp. 122–162.
- Lutjeharms, J.R.E., Cooper, J., 1996. Interbasin leakage through Agulhas current filaments. *Deep-Sea Research Part I* 43, 213–238.
- Lutjeharms, J.R.E., Catzel, R., Valentine, H.R., 1989. Eddies and other border phenomena of the Agulhas Current. *Continental Shelf Research* 9, 597–616.
- Lutjeharms, J.R.E., Cooper, J., Roberts, M., 2000. Upwelling at the inshore edge of the Agulhas Current. *Continental Shelf Research* 20, 737–761.
- Lutjeharms, J.R.E., Boebel, O., Rossby, H.T., 2003a. Agulhas cyclones. *Deep-Sea Research Part II* 50, 13–34.
- Lutjeharms, J.R.E., Penven, P., Roy, C., 2003b. Modelling the shear edge eddies of the southern Agulhas Current. *Continental Shelf Research* 23, 1099–1115.
- Matano, R.P., Beier, E.J., 2003. A kinematic analysis of the Indian/Atlantic interocean exchange. *Deep-Sea Research Part II* 50 (1), 229–249.
- Olson, D.B., 1991. Rings in the ocean. *Annual Review of Earth and Planetary Sciences* 19, 283–311.
- Olson, D.B., Evans, R.H., 1986. Rings of the Agulhas Current. *Deep-Sea Research* 33A (1), 27–42.
- Olson, D.B., Fine, R.A., Gordon, A.L., 1992. Convective modifications of water masses in the Agulhas. *Deep-Sea Research Part A—Oceanographic Research Papers* 39 (1A), S163–S181.
- Peeters, F.J.C., Acheson, R., Brummer, G.J.A., 2004. Vigorous exchange between the Indian and Atlantic oceans at the end of the past five glacial periods. *Nature* 430 (7000), 661–665.
- Peterson, R.G., Stramma, L., 1991. Upper-level circulation in the South Atlantic Ocean. *Progress in Oceanography* 26, 1–73.
- Richardson, P.L. (Ed.), 2003. Inter-ocean exchange around South Africa. *Deep-Sea Research Part II* 50, 1–319.
- Richardson, P.L., Garzoli, S.L., 2003. Characteristics of intermediate water flow in the Benguela current as measured with RAFOS floats. *Deep-Sea Research Part II* 50, 87–118.
- Richardson, P.L., Lutjeharms, J.R.E., Boebel, O., 2003. Introduction to the “inter-ocean exchange around southern Africa”. *Deep-Sea Research Part II* 50, 1–12.
- Schmid, C., Boebel, O., Zenk, W., Lutjeharms, J.R.E., Garzoli, S.L., Richardson, P.L., Barron, C., 2003. Early evolution of an Agulhas Ring. *Deep-Sea Research Part II* 46 (1–2), 355–392.
- Schouten, M.W., de Ruijter, W.P.M., Van Leeuwen, P.J., Lutjeharms, J.R.E., 2000. Translation, decay and splitting of Agulhas rings in the southeastern Atlantic Ocean. *Journal of Geophysical Research* 105, 21913–21925.
- Smith, W.H.F., Sandwell, D.T., 1997. Global sea floor topography from satellite altimetry and ship depth soundings. *Science* 277 (5334), 1956–1962.
- Smith, W.H.F., Wessel, P., 1990. Gridding with continuous curvature splines in tension. *Geophysics* 55 (3), 293–305.
- Valentine, H.R., Lutjeharms, J.R.E., Brundrit, G.B., 1993. The water masses and volumetry of the southern Agulhas Current region. *Deep-Sea Research Part I* 40 (6), 1285–1305.
- Van Ballegooyen, R.C., Gründlingh, M.L., Lutjeharms, J.R.E., 1994. Eddy fluxes of heat and salt from the southwest Indian Ocean into the southeast Atlantic Ocean: a case study. *Journal of Geophysical Research* 99 (C7), 14053–14070.
- Van Veldhoven, A., 2005. Observations of the evolution of Agulhas Rings. Doctoral Thesis, Royal Netherlands Institute for Sea Research (NIOZ), Texel, Netherlands. 157pp.
- Wessel, P., Smith, W.H.F., 1991. Free software helps map and display data. *EOS Transactions of the American Geophysical Union* 72, 445–446.